Development of direct compression Acetazolamide tablet with improved bioavailability in healthy human volunteers enabled by cocrystallization with *p*-Aminobenzoic acid

Nimmy Kumari[¥], Parag Roy[‡], Sukanta Roy[§], Chenguang Wang[†], Sourav Das[§], Noopur Pandey[‡], Susanta Kumar Mondal[†], Anirbandeep Bose[§], Changquan Calvin Sun^{†*} and Animesh Ghosh[¥]*

*Solid State Pharmaceutics Research Lab, Department of Pharmaceutical Sciences and Technology, Birla Institute of Technology, Mesra, Ranchi – 835215, Jharkhand, India.

§Bioequivalence Study Center, TAAB Biostudy Services, Ibrahimpore Road, Kolkata 700032, India

⁸School of Pharmacy, The Neotia University, Sarisha, West Bengal, Pin: 743368, India.

[♦]TCG Life Sciences Pvt. Ltd, Block-EP & GP, BIPL, Tower-B, Salt Lake, Sector-V, Kolkata, 700091, India.

[†]Pharmaceutical Materials Science and Engineering Laboratory, Department of Pharmaceutics, College of Pharmacy, University of Minnesota, 9-127B Weaver-Densford Hall, 308 Harvard Street S.E., Minneapolis, MN 55455, United States.

*Corresponding Authors:

1. Animesh Ghosh, PhD
Associate Professor
Department of Pharmaceutical Sciences and Technology,
Birla Institute of Technology, Mesra
Ranchi – 835215, Jharkhand, India
E-mail: aghosh@bitmesra.ac.in, anim 1607@yahoo.co.in

2. Changquan Calvin Sun, PhD
Professor and Associate Department Head
Department of Pharmaceutics,
College of Pharmacy
University of Minnesota,
9-127B Weaver-Densford Hall, 308 Harvard Street S.E
Minneapolis, MN 55455, United States
Email: sunx0053@umn.edu

ABSTRACT

Pharmaceutical cocrystallization has been widely used to improve physicochemical properties of APIs. However, developing cocrystal formulation with proven clinical success remains scarce. Successful translation of a cocrystal to suitable dosage forms requires simultaneously improvement of several deficient physicochemical properties over the parent API, without deteriorating other properties critical for successful product development. In the present work, we report the successful development of a direct compression tablet product of acetazolamide (ACZ), using a 1:1 cocrystal of acetazolamide with *p*-aminobenzoic acid (ACZ-PABA). The ACZ-PABA tablet exhibits superior biopharmaceutical performance against the commercial tablet, DIAMOX® (250 mg), in healthy human volunteers, leading to more than 50% reduction in the required dose.

Keywords: Acetazolamide (ACZ), *p*-aminobenzoic acid (PABA), Solubility, Caco-2 cell permeability, Tabletability, comparative bioavailability study

1. Introduction

15

16

17

18

19

20

21

22

23

24

25

26

27

28

29

30

31

32

33

34

35

36

37

38

39

40

41

42

43

44

45

Acetazolamide, 5-acetamido-1,3,4-thiadiazole-2-sulfonamide (ACZ), is a carbonic anhydrase inhibitor primarily used to treat glaucoma (Arenas-García et al., 2010; Fang et al., 2021) It is also used as an adjuvant therapy for epilepsy, diuresis, and high-altitude sickness, oedema caused by congestive heart failure, and preventing drug-related side effects in the treatment of influenza (Arenas-García et al., 2012) Given the many therapeutic benefits, World Health Organization (WHO) has included ACZ in the list of essential medicines.(Meers et al., 2020) However, being a Biopharmaceutical Classification System (BCS) class IV drug, ACZ suffers from both low solubility and low permeability (Pandey and Ghosh, 2022; Zhang et al., 2019). In addition, poor flowability and tabletability of ACZ affect its formulation development. (Di Martino et al., 2001; Kaur et al., 2002) To overcome these challenges, researchers have attempted various formulation strategies, including nanoparticles (Verma et al., 2013), microspheres (Haznedar and Dortunc, 2004), liposomes (El-Gazayerly and Hikal, 1997), inclusion complexes (Gladys E. Granero et al., 2008), spray drying(Di Martino et al., 2001) and cocrystals (Arenas-García et al., 2010; Manin et al., 2020; Meers et al., 2020). Over the years, pharmaceutical cocrystals have emerged as an important tool to improve the poor physicochemical properties of active pharmaceutical ingredients (APIs) without compromising their pharmacological activities.(Ji et al., 2022; Kale et al., 2017; Kumari et al., 2019; Wong et al., 2021; Yousef and Vangala, 2019) A main strength of cocrystallization lies in its wide range of applicability to improve physicochemical properties of APIs, thus providing an array of benefits at the same time. (Chow et al., 2012) Consequently, cocrystals have gained considerable interest from the pharmaceutical industry, academic institutions, and drug regulatory bodies across the world (Aitipamula et al., 2012; Kumari and Ghosh, 2020; Roy and Ghosh, 2020).

ACZ consists of a sulfonamide group, an acetamide and a thiadiazole group (**Figure 1**), which provides potential sites for non-covalent interactions with complementary coformers. Thus, many cocrystals of ACZ with various acidic and amide coformers were reported in literature, which are mostly focused on the preparative strategies and structural determination (Arenas-García et al., 2012, 2010; Bolla and Nangia, 2016; Kakkar et al., 2018), with limited evaluation of their physicochemical properties (Manin et al., 2020; Song et al., 2019; Zhang et al., 2019). Moreover, a majority of the reported coformers were not in the Generally Regarded As Safe (GRAS) list, making them less attractive for tablet formulation development. Furthermore, due to the poor

46 flowability and tabletability properties of ACZ, tablets are usually prepared using a resource-47 intensive wet granulation process instead of the more efficient direct compression process 48 (Duggirala et al., 2016; Huang, 2004; Karki et al., 2009; Schultheiss and Newman, 2009). Because 49 these stated problems can be addressed by modifying crystal packing (Aitipamula and Vangala, 50 2017; Sun, 2009), cocrystallization would provide an opportunity to simultaneously improve these 51 physicochemical properties to enable successful pharmaceutical tablet development (Arenas-52 García et al., 2017). In this context, it is also of great significance to explore the applicability of 53 cocrystals of ACZ in improving the biopharmaceutical properties. In this work, we systematically 54 evaluated the cocrystal of ACZ with p-amino benzoic acid (PABA), which could be prepared by 55 both mechanochemical and slurry-based sonication assisted method (Manin et al., 2020). The 56 ACZ-PABA cocrystal demonstrates improved aqueous solubility in comparison to ACZ and, 57 importantly, PABA is a GRAS listed coformer. In the present work, bulk ACZ-PABA cocrystal 58 was prepared using simplified slurry-based techniques and physicochemical properties, such as 59 permeability and tabletability, were studied. The improved tabletability of the ACZ-PABA led to 60 a successful development of an ACZ tablet by direct compression, which also exhibited an 61 excellent safety profile and comparative pharmacokinetic profiles in healthy human volunteers.

63 2. Materials and methods

64 **2.1.** *Materials*

62

73

65 Acetazolamide, 99.8% was obtained as a gift from Nakoda Chemicals Ltd. (Hyderabad, India). PABA, 99% was purchased from Sigma-Aldrich (St. Louis, Missouri, USA). 66 Microcrystalline cellulose (MCC, AVICEL® PH101) and Croscarmellose sodium (CCS, AC-DI-67 SOL®) was purchased from Signet Excipients Private Limited (Mumbai, India). Fumed silica 68 (CAB-O-SIL® M-5P) was purchased from Cabot Sanmar Limited (New Delhi, India). All other 69 70 inactive ingredients were of pharmaceutical grade. Solvents were purchased from Rankem 71 (Gurgaon, Haryana). All analytical chemicals and solvents were used as received without further 72 purification.

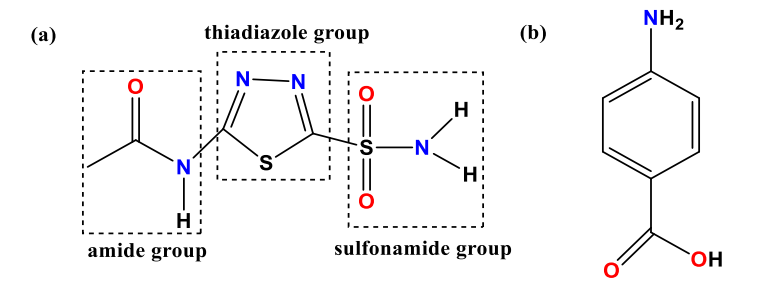


Figure 1. Molecular structures of (a) Acetazolamide (ACZ, MW= 222.245 g/mol) and (b) *p*-aminobenzoic acid (PABA, MW= 137.14 g/mol).

2.2. Methods

2.2.1. Preparation and characterization of ACZ-PABA cocrystal

An equimolar amount of ACZ (310 mg) and PABA (190 mg) was mixed with 2 mL ethanol in a round-bottom flask (50 mL). The mixture was stirred at 100 rpm for 6 h at room temperature. Ethanol was selected as the solvent as it is an International Conference on Harmonization (ICH) class 3 solvent (guideline 1).(Roy et al., 2023) The resultant suspension was filtered with a sintered funnel (porosity 4) and washed with ethanol and dried under vacuum at room temperature to give ACZ-PABA cocrystal as a white solid (460 mg, 92% yield). The powder X-ray diffraction (PXRD) pattern of the prepared powder was compared to the PXRD calculated from the reported ACZ-PABA crystal structure for confirming phase purity (**Figure S1**).

2.2.2. High performance liquid chromatography (HPLC) operating conditions

The concentrations of ACZ in the solutions samples were measured using an HPLC system (Thermo Fisher Scientific, UltiMate 3000) equipped with a photodiode array (PDA) detector. The HPLC system was controlled with workstation software Chromeleon 7 (version 7.2.10). A Syncronis C_{18} column (250 mm \times 4.6 mm ID, 5 μ m particle size, Thermo Scientific, India) was used. The chromatographic separation was achieved using a gradient method using acetonitrile (solvent A) and 0.1% (v/v) orthophosphoric acid (solvent B) as per the gradient program given in **Table S1**. The injection volume was 20 μ L and total run time was 12 min. A calibration curve was prepared in the linearity range of 2-16 μ g/mL and the absorbance of the eluents was monitored at a detection wavelength of 266 nm. No interference was observed between ACZ and PABA during HPLC measurements (**Figure S2**). Diluent used for sample preparation was acetonitrile and 0.1% (v/v) orthophosphoric acid in 85:15 (v/v) ratio.

2.2.3. Intrinsic Dissolution Studies

Intrinsic dissolution rate (IDR) study of ACZ and ACZ-PABA cocrystal was determined using a rotating disc method performed on a dissolution tester (TDT-08L, Electrolab, Mumbai, India). ACZ (200 mg) or ACZ-PABA (equivalent to 200 mg of ACZ) was compressed into a disc using a hydraulic press at a pressure of 2.5 tons per square inch for 5 min. Dissolution studies were performed in 900 mL of 0.01 N hydrochloric acid at 100 rpm, 37 ± 0.5 °C, as prescribed by the U.S. Pharmacopoeia. (K. Wang et al., 2022) Aliquots (2 mL) were withdrawn at specified time intervals, filtered through a 0.45 μ m membrane, and analyzed by HPLC after proper dilution to attain a concentration within that of the predetermined calibration curve. The IDR was calculated by dividing the slope of the linear region of a dissolution profile (R²> 0.99) with the surface area of the pellet (0.5 cm²).

111112

113

114

115

116

117

118

119

120

121

122

123

124

125

126

127

128

129

130

101

102

103

104

105

106

107

108

109

110

2.2.4. Caco-2 cell permeability studies

In vitro permeability studies using Caco-2 cell lines were performed for ACZ and ACZ-PABA cocrystal as per the experimental procedure previously reported (Yasmin et al., 2021). The Caco-2 human colon adenocarcinoma cell line was purchased from National Centre for Cell Science (Ganeshkhind Road, Pune, India). Following the standard cell culture procedure, Caco-2 cells were cultured in Dulbecco's Modified Eagle Medium (DMEM) containing 10% fetal bovine serum and antibiotics. All cells used in this study were between passages 38 to 50. Cells were plated in 96-well inserts (Corning, Sigma Aldrich, USA) and cultured for 21 days to reach confluence and cell differentiation. Initially, each insert containing the differentiated monolayers was carefully washed and filled with Hank's Balanced Salt Solution (HBSS with 10 mM HEPES, pH 7.4). The apical to basolateral ($A\rightarrow B$) permeability experiment was carried out in at 5 μ M concentration at 37 °C for 2.5 h without shaking under 5% CO₂ and 95% relative humanity (RH). Samples were collected from the receiver compartment and, along with initial samples from the donor compartment, diluted properly and analyzed using LC-MS/MS. The integrity of the monolayer was examined using Lucifer Yellow (LY) rejection assay. Wells with less than 1% fluorescence intensity in relation to the Lucifer yellow dosing solution were deemed satisfactory. All experiments were performed in triplicate and the apparent permeability coefficients (P_{app}) was calculated using Equation (1) (van Breemen and Li, 2005),

131
$$P_{app} = V_r \times \frac{dC}{dt} \times 1/AC_0 \qquad \text{Eq. (1)}$$

where, Vr is the volume of the recipient compartment, dC/dt is the slope of the cumulative concentration of the compound in the recipient chamber over time, A is the membrane surface area, and C_0 is the compound initial concentration in the donor chamber (van Breemen and Li, 2005).

2.2.5. Microscopy

Crystals dispersed in silicone oil were observed under a polarized light microscope (Eclipse e200; Nikon, Tokyo, Japan) equipped with a DS-Fi1 microscope digital camera for capturing digital images (Hu et al., 2020).

2.2.6. Dynamic Vapor Sorption isotherm (DVS)

Water sorption isotherms of the materials were obtained using an automated vapor sorption analyzer (Intrinsic DVS, Surface Measurement Systems Ltd., Allentown, PA) at 25 °C. The nitrogen flow rate was 50 mL/min. Each sample was first dried with dry nitrogen purge until a constant weight was obtained. Then, the sample was exposed to a series of RH from 0% to 95% with the step size of 5% RH. At each specific RH, the equilibration criterion of either dm/dt ≤0.002% or maximum equilibration time of 6 h was applied. RH was changed to the next target value once one of the criteria was met (Wang et al., 2017).

2.2.7. Powder Flowability

Powder flowability was measured using a ring shear cell tester (RST-XS; Dietmar Schulze, Wolfenbüttel, Germany) with performance verified using a limestone powder standard. A 10 mL cell was used for collecting data at the pre-shear normal stress of 3 kPa using the 230 methods. From the shear cell measurements, powder flowability index (*ff*_c) was calculated (Wang et al., 2017).

2.2.8. Tabletability

A compaction simulator (Styl'One Evolution; MedelPharm, Beynost, France) using a symmetrical, force-controlled, extended compression cycle with a dwell time of 3 s was used for tabletability assessment of ACZ and ACZ-PABA powders with external lubrication (Vreeman and Sun, 2021). Round, flat-faced tooling with an 8 mm diameter was used to compress tablets. Tabletability of formulated powders was assessed by simulating a Korsch XL100 tablet press at 50 rpm, corresponding to a production speed of 12,000 tablets/h. Tablet diametrical breaking force

was measured under ambient conditions (22 °C and 32% RH) using a texture analyzer (TA-XT2i;

164 Texture Technologies Corporation, Scarsdale, NY), with a speed of 0.01 mm/s. Tablet dimensions

were measured using a digital caliper (Mitutoyo Corp, Kanagawa, Japan). Tablet tensile strength

166 (σ, MPa) was calculated using Equation (2) (Song et al., 2021).

$$\sigma = 2F/\pi Dh \qquad \text{Eq. (2)}$$

Where F is breaking force (N), D (mm) and h (mm) are diameter and thickness of the ejected

tablet, respectively.

170171

2.2.9. Stability

Stability study of ACZ-PABA cocrystal was carried out at storage conditions of 40 ± 2 °C,

 $75\% \pm 5\%$ RH in a stability chamber (Thermolab Scientific Equipments, Mumbai, India). The

samples (~200 mg) were stored in an open-cap glass vial (10 mL) and withdrawn after 5, 9 and 13

weeks and analyzed for physical stability by PXRD, and chemical stability by HPLC.

176

177

179

180

181

182

174

175

2.2.10. Cocrystal-excipient compatibility

The excipient compatibility of the ACZ-PABA cocrystal was studied using binary physical

mixtures containing ACZ-PABA cocrystal and individual excipients, which were prepared in a 1:1

(w/w) ratio by geometric mixing. The prepared mixtures were kept at 40 ± 2 °C and $75 \pm 5\%$ RH

in a stability chamber (Thermolab Scientific Equipments, Mumbai, India) for 7 days (Koranne et

al., 2019). Samples were analyzed by DSC and PXRD for signs of possible incompatibility.

183

184

185

186

187

188

189

190

191

192

193

2.2.11. Formulation of ACZ-PABA tablet

Tablets comprising ACZ-PABA (equivalent to 250 mg ACZ) and different excipients were manufactured by using a direct compression process. Firstly, all ingredients except magnesium stearate (MgSt) were manually mixed for 10-15 min. The powder mixture was then passed through an ASTM sieve (mesh size #60 and screen aperture 250 µm) six times to make sure all large agglomerates of fumed silica were broken. Finally, the powder mixture was mixed for another 5 min. MgSt was then added and mixed for 2 min to obtain the final blend, which was manually introduced into the die and compressed in a rotary tablet press (CADMACH, Ahmedabad, India), using a 13 mm round and beveled edge punch to obtain 750 mg tablets. Disintegration time, uniformity of weight, uniformity of content, friability, tablet strength and thickness were measured

for ACZ-PABA tablets as per the standard methods prescribed in Indian Pharmacopoeia (Silchenko et al., 2020). The thickness of tablets was measured using a digital vernier caliper (Classic Digimatic Caliper, Classic Corporation, Ahmedabad, Gujrat); breaking force of tablets was checked by a tablet hardness tester (Electrolab Pvt. Ltd., Mumbai, India); and friability was measured as the percent mass loss in a Roche friabilator (EF-2, Electrolab Pvt. Ltd., Mumbai, India). Disintegration time of ACZ-PABA tablets was measured in basket-rack assembly containing six tubes (Disintegration Tester, ED-2L, Electrolab Pvt. Ltd., Mumbai, India), suspended in a 1 L beaker containing water maintained at 37 ± 2 °C.

2.2.12. In-vitro dissolution study

In-vitro dissolution study of ACZ-PABA cocrystal tablets and reference tablets (DIAMOX® 250 mg) was performed in a USP type II dissolution apparatus (Electro Lab TDT-08L, Mumbai, India). The rotational speed of paddle was 100 rpm and the dissolution media (900 mL) was maintained at 37 ± 0.5 °C. Dissolution was performed in four different media, 0.01 N hydrochloric acid (prescribed by U.S. Pharmacopoeia), pH 4.5 acetate buffer, and pH 6.8 and pH 7.4 phosphate buffers. Six tablets from each set of tablets were used in each medium. Samples were withdrawn at predetermined time points, filtered using syringe filters (0.45 μ m) and concentration of the drug was determined using HPLC after proper dilution from the predetermined calibration curve. The dissolution data obtained were plotted as cumulative drug released vs, time.

2.2.13. Sub-chronic oral toxicity study

The sub-chronic oral toxicity of ACZ-PABA cocrystal was conducted at TAAB Biostudy Services (Jadavpur, Kolkata, India) in accordance with Schedule "Y" Drugs and Cosmetics (Amendment) Rule, Ministry of Health and Family Welfare, Government of India and in the spirit of OECD Principles of Good Laboratory Practices. Prior to the initiation of the study, the study protocol was approved by the Institutional Ethics Committee of TAAB Biostudy Services, Jadavpur, Kolkata, India. Forty-eight healthy Wistar rats, i.e., 24 males and 24 females (nulliparous and not pregnant), weighing 150 to 200 g, were randomly selected, and divided into four groups, each group containing 6 rats of either sex. All animals were kept in polycarbonate cages at 20-24 °C and 30–70% RH in a 12 h light/dark cycle and supplied with standard laboratory

food and water *ad libitum* according to CPCSEA guidelines. (Soni et al., 2018) Seven days prior to the initial dosing, animals were allowed to get acclimatized to laboratory conditions. Thereafter, the cocrystals were orally administered at a dosing regimen of 25 mg/kg, 50 mg/kg, and 100 mg/kg (low dose, medium dose, and high dose) to each group of animals according to the randomization and treatment schedule (**Table S2**).

All animals were observed daily for the emergence of any clinical symptoms and twice daily for mortality until the completion of the study. The body weights of individual animals were recorded initially and thereafter weekly. The amount of food consumed by each rat in each group was recorded weekly, and the food intake per rat for the control and treated groups was determined. The haematological and serum biochemical parameters of all groups were measured and compared with those of the control group. (Dan et al., 2016) Upon completion of the study on the 29th day, all animals were sacrificed by cervical dislocation. The vital organs (heart, kidneys, liver, and stomach) were isolated from the control and treated groups and preserved in 10% formalin solution for histopathological examinations. (Singh and Kumar, 2011) The haematological parameters were determined using a Medonic M Series Cell Counter (LABX, Thiruvananthapuram, Kerala, India) and the serum biochemical parameters were determined using a MICROLAB-300 Semi-Auto Analyzer (Biozone India Scientific, New Delhi, India).

2.2.14. Study Design, Dosing and Blood sampling

The comparative oral bioavailability of ACZ-PABA cocrystal tablet (Batch No: BIT2021) was conducted in healthy human volunteers against the reference DIAMOX® IR tablets (250 mg, Batch No: GTC2183A). This randomized, open-label, single dose study (two-period cross over design) was conducted at the Clinical Pharmacology Unit of TAAB Biostudy Services (CDSCO approved Bioequivalence Study Centre, Kolkata, India) in accordance with the revised principles of World Medical Association's Declaration of Helsinki 2008. Prior to this, the protocol of the study was approved by Human Ethics Committee (Hurip Independent Bioethics Committee, Kolkata, India), Protocol No. 12/21/AC and written Informed Consent Form for participation in the study was obtained from all the volunteers. Six healthy male volunteers (Age: 35 ± 2.16 Yrs; BMI: 23.55 ± 1.87 Kg/m²) were selected for each arm of this study. Each tablet was taken by a volunteer in the morning after 10 h of fasting. Blood samples were collected at predetermined time points, 0 (pre-dose), 0.5, 1.0, 1.5, 2.0, 3.0, 4.0, 6.0, 8.0, 10.0, 12.0, 14.0, 16.0, 24.0 h (post dose)

in 5 mL K₂EDTA vacutainers via an indwelling catheter placed in one of the forearm veins. Heparin-lock technique was used to prevent clotting of blood in the indwelling catheter. Before each blood sample was drawn through the catheter, 0.5 mL of blood was discarded to purge the heparinised blood sample in the catheter. Blood samples were centrifuged at 10,000 rpm at 4 °C, plasma was collected and stored at -70°C in polyethylene tubes till further analysis.

2.2.15. Bioanalytical method development

The LC-MS/MS system (API 2000TM, AB SCIEX, Foster, CA) was used for determining the concentration of ACZ in human plasma. Chromatographic separation was achieved on a Kinetex[®] C18 100A column (50 x 3 mm, 5μm, Phenomenex, India), using gradient elution mode with mobile phase containing 0.1% (v/v) formic acid in Milli-Q water (Solvent A) and 0.1% (v/v) formic acid in acetonitrile (Solvent B) at the flow rate of 0.5 mL/min. The injection volume was 10 μL and the total run time was 7 min. Quantification of the ACZ was done in negative ion detection mode using a triple quadrupole mass spectrometer (MS-MS), equipped with turbo spray ionization source. Multiple reaction monitoring (MRM) mode was utilized throughout the scan with parent ion/product ion transition pairs of 220.7/83.0 for ACZ and 269/170.2 for tolbutamide as internal standard (IS), respectively, with a dwell time of 200 ms per transition. The parent and product ion mass spectra of ACZ and IS are shown in **Figure S3-S6**. Analyst[®] 1.6.2 (AB SCIEX) software was used for data acquisition and instrument control. The final MRM scan of analyte and IS spiked in blank plasma is provided in **Figure S7**.

Stock solutions of both analyte (ACZ) and IS (Tolbutamide) of 1 mg/mL were prepared by dissolving corresponding compounds in DMSO and kept in deep freezer (Celfrost, Chennai, India) at -20 °C for further sample preparation. Afterwards, stock solutions were further diluted to obtain the working standard of 1 µg/mL using organic solvent used in mobile phase. System suitability and instrumental tuning were carried out with prepared working standards. Calibration concentrations of 78.13, 156.25, 312.5, 625, 1250, 2500, 5000, 10000 and 20000 ng/mL of analyte was prepared from working standard spiked in blank plasma with a known concentration of IS (10 ng/mL) to obtain the calibration curve. Different quality control (QC) concentrations were prepared for concurrent validation of precision accuracy (PA) batch and plasma analysis.

Frozen plasma samples were first thawed at room temperature and plasma extraction was performed by protein precipitation technique. 100 μ L of plasma was taken and precipitated with 400 μ L of acetonitrile containing 10 ng/mL of tolbutamide (IS) and vortexed for 10 min followed by centrifugation for 10 min at 10,000 rpm at 4 °C. 300 μ L of supernatant was taken, filtered using syringe filter (0.45 μ m) and diluted 10 times, then transferred into auto sampler vials for injection.

2.2.16. Pharmacokinetic analysis

The plasma concentration vs. time profiles of ACZ for each subject was analysed by non-compartmental analysis using the PK Functions (pK₁ and pK₂) for Microsoft Excel to obtain different pharmacokinetic parameters, i.e., maximum plasma concentration (C_{max}), time to reach maximum plasma concentration (T_{max}), elimination half-life ($T_{1/2}$), area under the curve for plasma concentration from zero to the last measurable plasma sample time (AUC_{0-t}), area under the curve for plasma concentration from zero to time infinity (AUC_{0-∞}) and elimination rate constant (K_{cl}).

2.2.17. Statistical analysis

ANOVA (subject, period, treatment) and 90 % confidence interval (CI) was applied to C_{max} , Ln C_{max} , AUC₀₋₂₄, Ln AUC₀₋₂₄, AUC_{0- ∞} and Ln AUC_{0- ∞}. Differences and ratios of C_{max} , Ln C_{max} , AUC₀₋₂₄, Ln AUC_{0- ∞} and Ln AUC_{0- ∞} were also calculated for the test formulation.

3. Results and discussion

3.1. Solubility and phase stability

The reported solubility (S_{CC}) of ACZ-PABA cocrystal at pH 2.0 (9.0 x10⁻³ mol. L⁻¹) and pH 7.4 (1.5 x10⁻² mol. L⁻¹) has a solubility advantage (SA) of 2.5 and 4.1 times over the solubility of ACZ in the respective buffer solutions (Manin et al., 2020). The significantly higher solubility of cocrystal suggests a potentially higher concentration of ACZ throughout the gastrointestinal tract, resulting in improved bioavailability. As per the regulatory guidelines provided by US-FDA, substantial dissociation of the API from the cocrystal is essential before reaching the site of action (Roy et al., 2022). Phase stability studies of ACZ-PABA were performed by suspending the cocrystal in various buffer media for 24 hours with continuous shaking. Solid residues after 24 h suggests partial dissociation of the cocrystal into ACZ (**Figure S8**).

3.2. Intrinsic dissolution rate

Compared to the equilibrium solubility, intrinsic dissolution rate (IDR) can more reliably predict bioavailability of cocrystals that dissociate in the solution media during the course of prolonged equilibration (Manin et al., 2020). From the linear region of the dissolution curve, IDR value of ACZ-PABA (18.9 mg cm⁻² min⁻¹) is 1.15 times that of ACZ (16.4 mg cm⁻² min⁻¹) in 0.01 N hydrochloric acid. The 15% improvement in IDR is lower than the reported 2.5 fold enhancement in solubility. This is likely due to dissociation of ACZ-PABA into less soluble ACZ during the course of IDR experiment, which partially covered the surface of the pellet to cause slower dissolution.

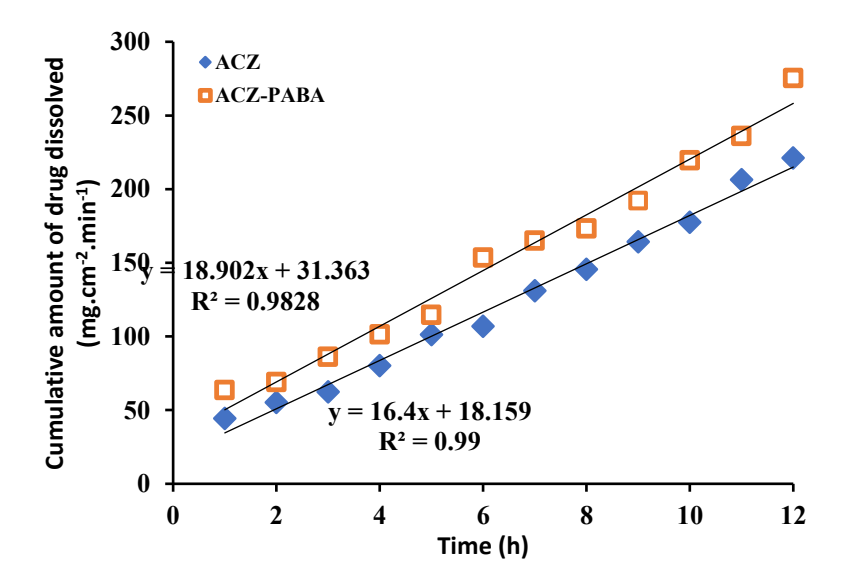


Figure 2. Intrinsic dissolution profiles of ACZ and ACZ-PABA in 0.01 N hydrochloric acid at 37 \pm 0.5 °C.

3.3. Caco-2 cell permeability studies

Orally administered drugs must have adequate oral bioavailability in order to attain their therapeutic effectiveness. Being a Biopharmaceutics Classification System (BCS) class IV drug, ACZ has both low solubility and low permeability (Ghadi and Dand, 2017; G.E. Granero et al., 2008). Thus, the ability of ACZ to cross the cell membrane is a critical factor for attaining adequate bioavailability.

The $P_{\rm app}$ value for ACZ from apical to basolateral $P_{\rm app}$ (A \rightarrow B), 0.85 × 10⁻⁶ cm.s⁻¹, is significantly increased to 1.35 × 10⁻⁶ cm.s⁻¹, for the ACZ-PABA cocrystal (**Table 1**), suggesting

an improved permeability of the cocrystal. Both the higher permeability and increased solubility of the cocrystal suggests the potentially improved bioavailability of the cocrystal.

Table 1. Main physicochemical and biopharmaceutical parameters of ACZ and ACZ-PABA cocrystal.

Materials	IDR (mg.cm ⁻² .min ⁻¹)	$P_{\rm app}$ (A \rightarrow B) (×10 ⁻⁶ cm.s ⁻¹)
		A-B ^a
ACZ	16.4	0.85 ± 0.05
ACZ-PABA	18.9	1.35 ± 0.05

3.4. Microscopy

Both ACZ (**Figure 3a**) and ACZ-PABA (**Figure 3b**) samples showed birefringence, which is consistent with their crystallinity demonstrated by their PXRD patterns. Crystals in both samples were irregularly shaped and their particle size distributions are approximately in the same range (Figure 3).

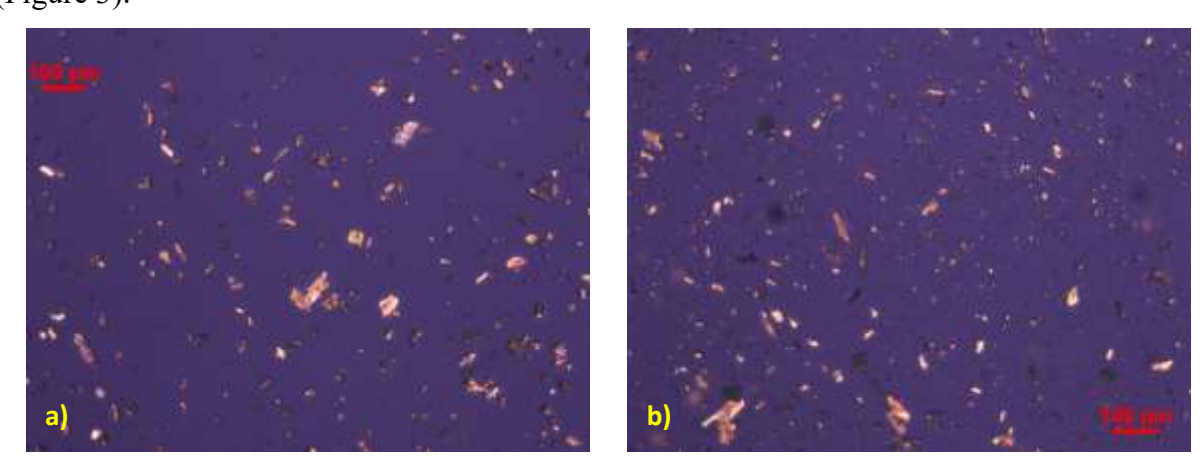


Figure 3. Polarized light microscopic images of a) ACZ and b) ACZ-PABA.

3.5. Dynamic Vapor Sorption Isotherm

Dynamic vapor sorption analysis revealed slightly higher water sorption than that of ACZ (**Figure 4**). However, only 0.25% moisture is adsorbed by the ACZ-PABA cocrystal at 80% RH. Thus, ACZ-PABA cocrystal is considered non-hygroscopic and moisture induced physical phase change was not expected during the manufacturing and storage of ACZ-PABA formulations.

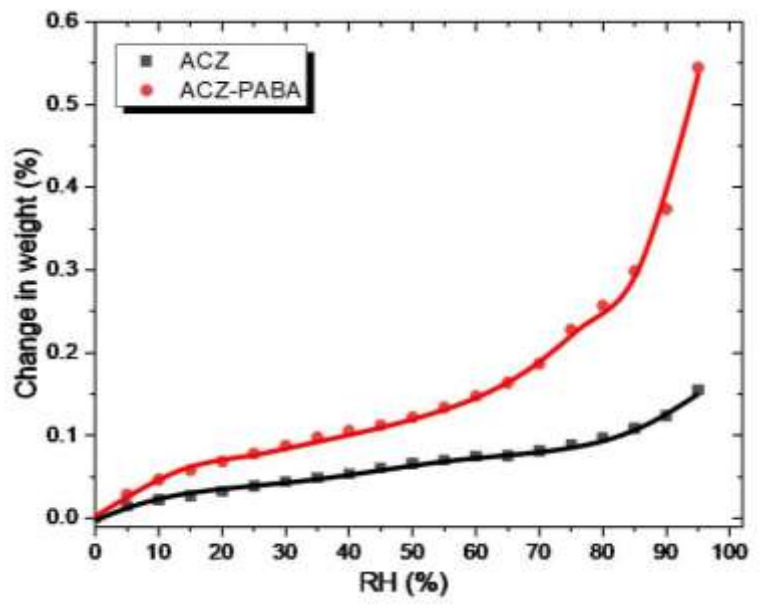


Figure 4. Moisture sorption isotherm of ACZ and ACZ-PABA at 25 °C.

3.6. Powder Flowability and Tabletability

The flowability, measured by the *ff*c value, of ACZ (ffc = 4.2) is approximately the same as that of ACZ-PABA cocrystal (ffc = 4.1). This is consistent with their approximately similar crystal sizes and shape (**Figure 3**). The flowability of ACZ-PABA cocrystal is poorer than that of Avicel PH102, which is a material exhibiting borderline flowability for high speed tableting. Therefore, flowability enhancement is expected when preparing a high dose direct compression formulation using ACZ-PABA cocrystal. We addressed this challenge by using dry nano-coating with fumed silica (Sun, 2010; C. Wang et al., 2022; Zhou et al., 2013, 2012). The tabletability of ACZ-PABA cocrystal is profoundly better than that of ACZ up to 200 MPa compaction pressure (**Figure 5**). ACZ could only form intact, but very weak tablets, at ~120 MPa while no intact tablets could be formed at all other pressures. In contrast, ACZ-PABA cocrystal could form intact tablets at all pressures up to 200 MPa. In this pressure range, tablet mechanical strength increased with increasing pressure up to 1.7 MPa. Above 200 MPa, ACZ-PABA cocrystal suggests the possibility of developing a direct compression tablet formulation using the cocrystal.

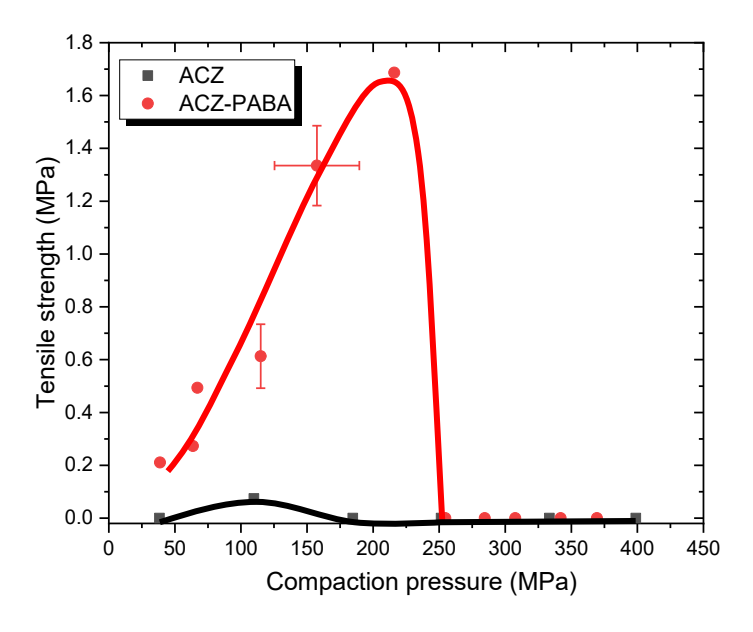


Figure 5. Tabletability profiles of ACZ and ACZ-PABA cocrystal.

3.7. Stability

The stability of ACZ-PABA cocrystal at stress condition (40 ± 2 °C, $75 \pm 5\%$ RH) was performed to check for any kind of dissociation or phase transformation under stressed conditions. Even after 13 weeks of storage, ACZ-PABA cocrystal showed no signs of solid form change based on its PXRD pattern (**Figure 6**). The HPLC analysis also confirmed no increased level of impurities of the cocrystal (**Figure S9**).

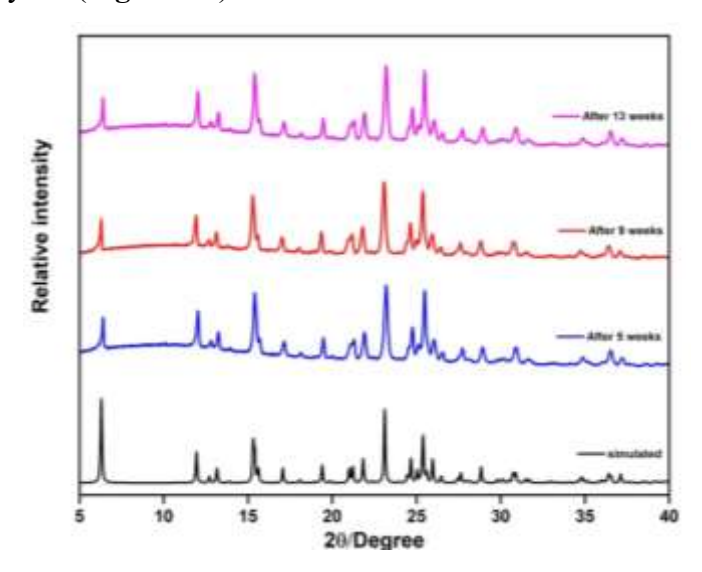


Figure 6. PXRD pattern of samples from accelerated stability experiments in comparison to the initial cocrystal sample.

3.8. Cocrystal-excipient compatibility

The compatibility of ACZ-PABA cocrystal with excipients was probed using DSC and PXRD. The DSC thermograms (Figure 7) demonstrated that the melting endotherm of the ACZ-PABA cocrystal at 217 °C remained unchanged in the presence of these excipients in stress conditions and no additional thermal events were observed, indicating an absence of intermolecular interactions between the cocrystal and these excipients up to the melting temperature. Further, the PXRD patterns of the ACZ-PABA cocrystal and its 1:1 physical mixture with excipients (Figure 8) showed no changes in the reflection peaks of cocrystal. The physical mixture containing MgSt is a mixed pattern of magnesium stearate (*) and the cocrystal. Some of the peaks of excipients were present in the physical mixtures, the peak positions of cocrystal peaks remain unchanged. Thus, DSC and PXRD analysis revealed that the cocrystal is compatible with these excipients, showing no disproportionation during storage under accelerated conditions. Therefore, these excipients were considered suitable for use in the tablet formulation containing ACZ-PABA cocrystal.

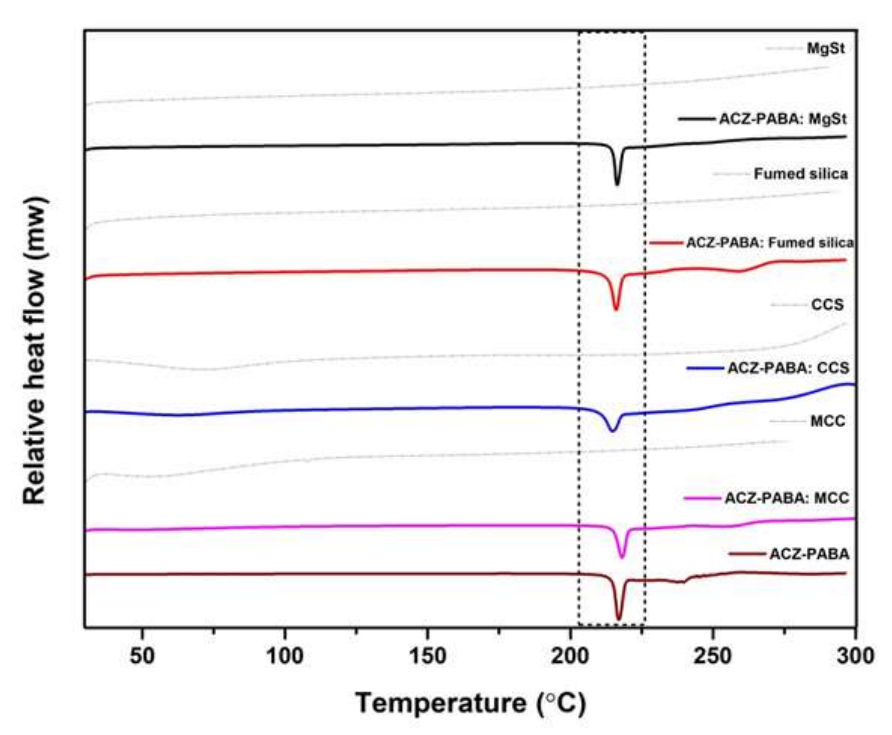


Figure 7. DSC heating curves of the ACZ-PABA cocrystal and its physical mixture (1:1 w/w) with different excipients (microcrystalline cellulose (MCC), croscarmellose sodium (CCS), fumed silica and magnesium stearate (MgSt).

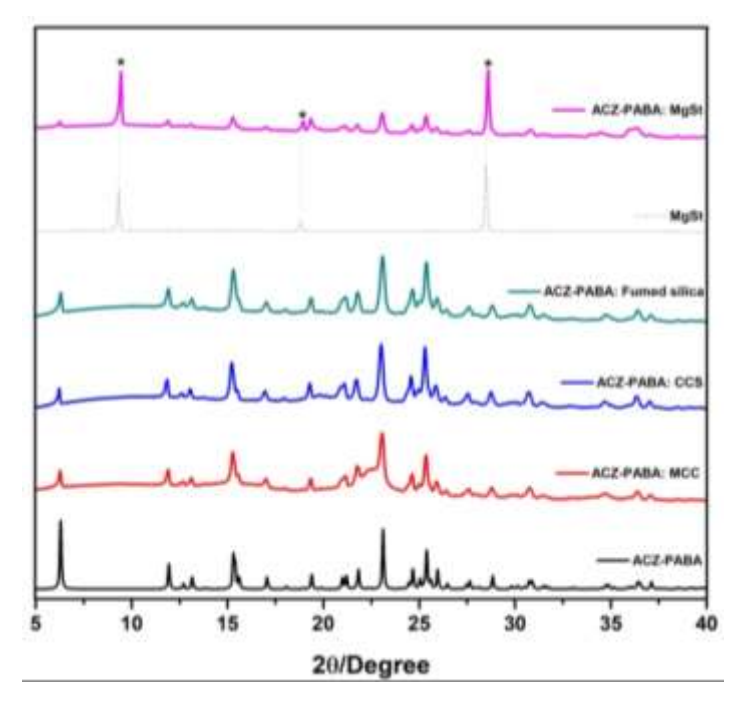


Figure 8. Overlay of powder patterns of ACZ-PABA cocrystal and its physical mixture (1:1 w/w) with different excipients (microcrystalline cellulose (MCC), croscarmellose sodium (CCS), fumed silica and magnesium stearate (MgSt).

3.9. Formulation of ACZ-PABA cocrystal tablet by direct compression method

ACZ is a candidate with poor flowability and tabletability, which ultimately affects its manufacturability. The ACZ-PABA cocrystal showed improved tabletability, enabling us to explore a direct compression tablet manufacturing process. Direct compression has several advantages over wet granulation, including fewer operating steps, less power use, less space, less time, and less labor, all of which contribute to lower tablet production costs. In the case of tablets of poorly soluble APIs, such as ACZ in the present study, directly compressed tablets release API particles upon disintegration, rather than granules. This translates to more rapid dissolution than that from a tablet prepared by wet granulation. With this impetus, ACZ-PABA cocrystal tablet was prepared with excipients designed for direct compression (Table 2). As mentioned earlier, the use of fumed silica in this formulation is intended to improve the flowability of the formulation given the poor flowability of ACZ-PABA cocrystal. All in-process quality control parameters, performed as per the standard Pharmacopeial method, are summarized in Table 3.

Ingredients	Function	Amount per tablet (mg)	Percent (%)
ACZ-PABA cocrystal	API	404 (~250 mg ACZ)	53.87
Microcrystalline cellulose	Filler/binder	297.25	39.63
(AVICEL® PH-101)			
Croscarmellose sodium	Disintegrant	37.5	5.00
$(AC-DI-SOL^{\mathbb{R}})$			
Fumed silica	Glidant	7.5	1.00
(CAB-O-SiL® M-5P)			
Magnesium stearate	Lubricant	3.75	0.50
Total		750	100

431
 432 **Table 3.** Physicochemical characterization of DIAMOX® and ACZ-PABA cocrystal tablet (250 mg ACZ).

430

Characteristics	DIAMOX®	ACZ-PABA
		Cocrystal Tablet
Product Image	BINNON	
Appearance	White colour capsule shape tablet	White colour round shape
	debossed with "DIAMOX" on the	bevelled edge tablet having
	upper surface, having one break	one break line on upper
	line on the lower surface.	surface.
Thickness (mm)	5.37 ± 0.05	4.06 ± 0.02
Hardness Average (kg/cm ²)	7.88 ± 0.23	21.61 ± 1.11
Disintegration time(min)	5-7 min	< 1 min
Friability (%)	0.18	0.13

3.10. In-Vitro drug release study

In-vitro drug release profile of ACZ from DIAMOX® (reference formulation) and ACZ-PABA cocrystal tablet (test formulation) in various media, 0.01 N hydrochloric acid, pH 4.5 acetate buffer and pH 6.8 and pH 7.4 phosphate buffers, are shown in **Figure 9**. The test formulation containing ACZ-PABA cocrystal showed superior dissolution behavior over the reference formulation over the entire pH range. Approximately 85% of the ACZ was released in the first 5 min of dissolution, which is considerably faster than the reference formulation (approximately 30% in 5 min). The faster dissolution of the test formulation is consistent with the improved solubility and IDR of ACZ-PABA cocrystal and the faster disintegration of the ACZ-PABA tablet (Table 3). The enhanced in vitro drug release encouraged us to further explore its potential improvement in oral bioavailability in humans.

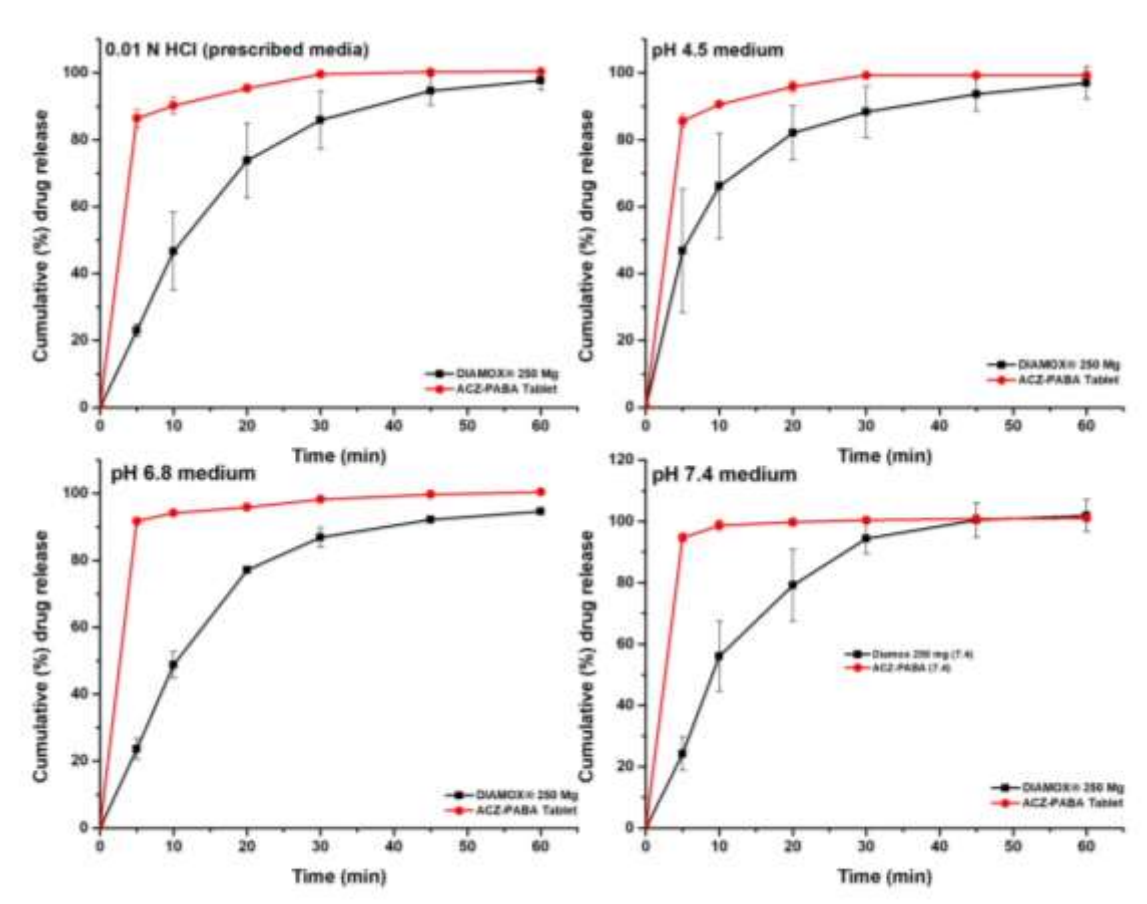


Figure 9. *In-Vitro* dissolution profile at 37 ± 0.5 °C for ACZ from DIAMOX® and ACZ-PABA cocrystal tablet in (a) 0.01 N Hydrochloric acid, (b) pH 4.5 (c) pH 6.8 and (d) pH 7.4. Each point represents mean \pm SD of six measurements (n = 6).

3.11. Sub-chronic oral toxicity study

The weight variability of male and female animals of each treatment group is represented in **Tables S3-S4**. The group mean body weight of low, middle, and high dose groups of animals showed no drastic weight reduction during the dosing period when compared to the control group. The group mean food consumption of different dose groups for 28 days of the study period (**Tables S5-S6**) did not show any abnormality or reduction in food intake. The hematological and serum biochemical analysis reports of male and female animals of each treatment group after study period (**Tables S7-S10**) showed no significant changes when compared with control and values obtained were within normal biological and laboratory limits. The histopathological images of the vital organs like heart, liver, kidney, and stomach of animals from high dose groups revealed no signs of abnormality (**Figure 10**).

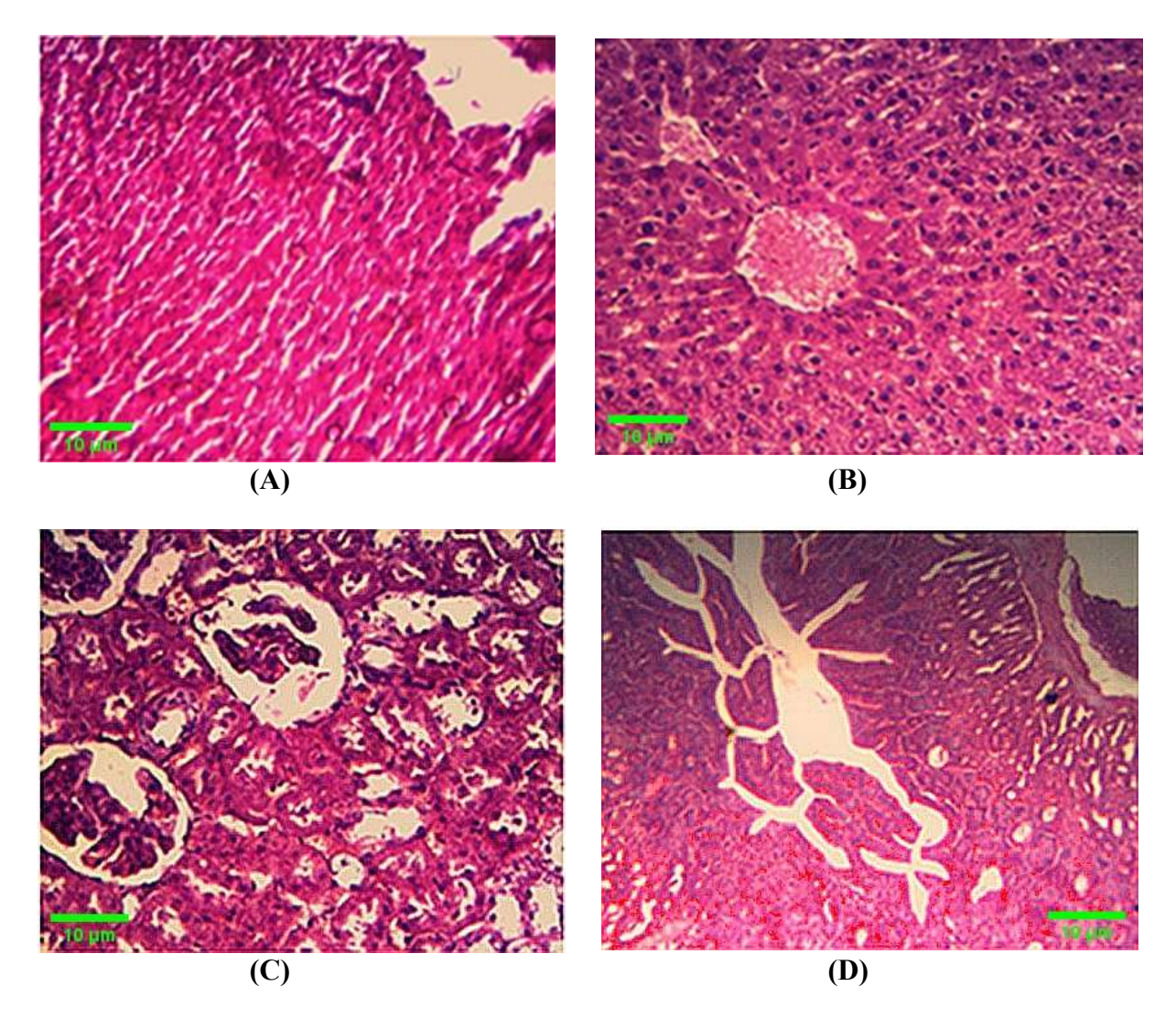


Figure 10. Histopathological images of the vital organs (a) Heart, (b) Liver, (c) Kidney, and (d) Stomach in experimental group of animals.

3.12. Pharmacokinetic studies in Healthy Human Volunteers

To investigate the effect of enhanced solubility and permeability of ACZ-PABA cocrystal on its bioavailability, a comparative bioavailability study was conducted in healthy human volunteers using both the test (ACZ-PABA cocrystal) and reference (DIAMOX®) tablets. The pharmacokinetic parameters (**Table 4**) and mean plasma concentration vs. time profile (**Figure 11**) revealed that the C_{max} (15123.96 ± 796.21 ng/mL) and AUC (86168.86 ± 3369.00 ng·h/mL) values for the test formulation were both significantly higher than the C_{max} (8199.22 ± 427.29 ng/mL) and AUC (35786.82 ± 4721.29 ng·h/mL) of the reference formulation. We attribute the higher C_{max} and AUC values of the test formulation to the synergistic effects of both enhanced

solubility and improved permeability as discussed earlier. The plasma concentration of ACZ for the test formulation was higher compared to the reference formulation at all the time points. The T_{max} of the test formulation is also shorter than the reference formulation, which could be attributed to the faster dissolution rate of the test formulation than the reference formulation. Other important pharmacokinetic parameters, i.e., C_{max} , Ln C_{max} , AUC₀₋₂₄, Ln AUC₀₋₂₄, AUC_{0-∞} and Ln AUC_{0-∞}, of test and reference formulations are given in **Tables S11-S16**. Based on the ANOVA (subject, period, treatment) analysis, none of the pharmacokinetic parameters was within the bioequivalence limit (**Table S17**). However, the bioavailability of the test tablets exhibits more than doubled bioavailability (238.38%) than that of the reference tablet in the same strengths. Thus, the prescribed dose of ACZ (250 mg) in the currently marketed tablet can likely be reduced by more than half using the ACZ-PABA cocrystal tablet, leading to significant reduction of dose. It should be noted that, despite the higher plasma concentration using the ACZ-PABA cocrystal tablet, no unwanted side effects were observed in the human volunteers during the pharmacokinetic studies.

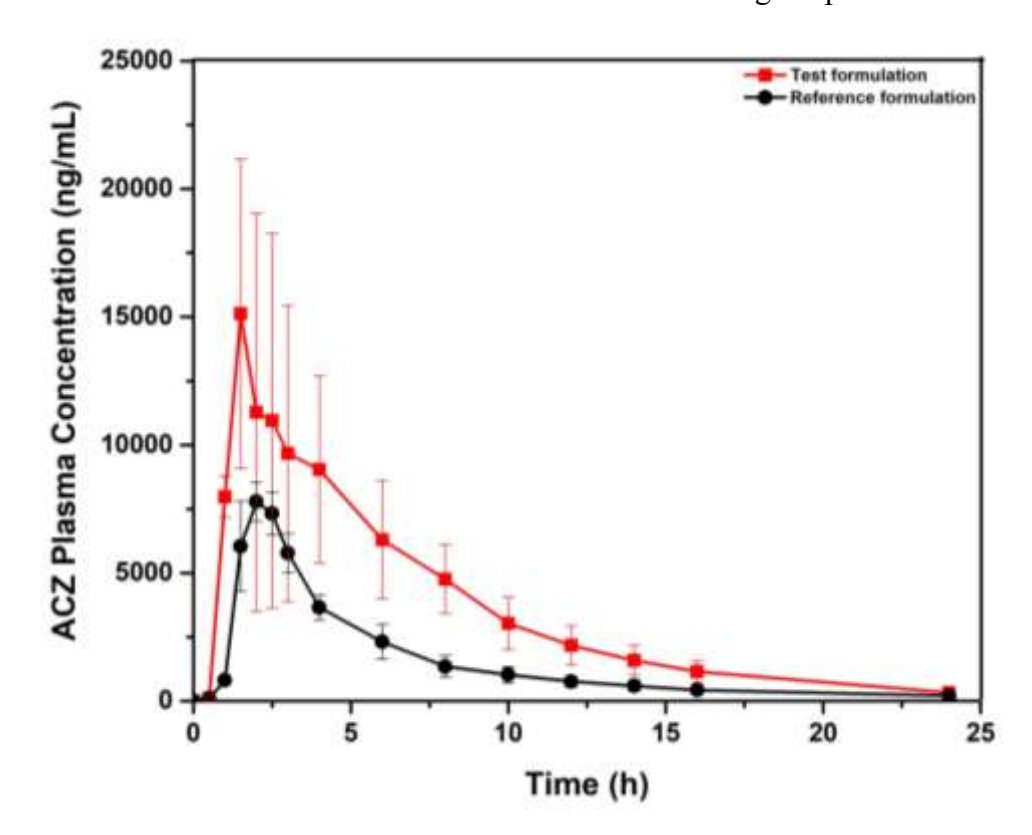


Figure 11. Mean (SD) plasma concentration- time profile of Acetazolamide (ACZ) after oral administration of ACZ-PABA cocrystal tablet (test formulation, red squares) and DIAMOX® (reference formulation, black circles) in healthy human volunteers.

Table 4. Pharmacokinetic comparison of Acetazolamide (ACZ) after oral administration of ACZ-PABA cocrystal tablet and DIAMOX[®] in healthy human volunteers.

Pharmacokinetic	Reference formulation		Test formu	Test formulation	
parameters	(DIAMOX®)		(ACZ-PAB	A Cocrystal Tablet)	
C _{max} (ng/mL) ^a	Mean	8199.22	Mean	15123.96	
	\pm SD	427.29	± SD.	796.21	
$T_{\max}(\mathbf{h})^{\mathbf{b}}$	Mean	2.17	Mean	1.50	
	\pm SD	0.26	± SD.	0.00	
$AUC_{0\text{-}24}(ng.h/mL)^c$	Mean	35786.82	Mean	86168.86	
	\pm SD	4721.29	± SD.	3369.00	
$AUC_{0\infty}(ng.h/mL)^d$	Mean	36960.40	Mean	89619.22	
	\pm SD	5168.62	± SD.	4427.81	
$k_{el}(h^{-1})^e$	Mean	0.18	Mean	0.17	
	\pm SD	0.02	± SD.	0.00	
$t_{1/2}\left(h\right)^{f}$	Mean	3.99	Mean	4.19	
	\pm SD	0.39	\pm SD.	0.14	
Relative	100%		238.38%		
Bioavailability (%)					

Data represented as mean \pm SD (n=6). ${}^aC_{max}$: maximum plasma concentration, ${}^bt_{max}$: time required to reach mean plasma concentration, ${}^cAUC_{0-24}$: Area under the plasma concentration-time curve at 0-24 h, ${}^dAUC_{0-\infty}$: Area under the plasma concentration-time curve at 0- ∞ h, ${}^ek_{el}$: elimination half-life, ${}^ft_{1/2}$: half life.

4. Conclusions

In this work, we present a case where a pharmaceutical cocrystal successfully modulated the physicochemical characteristics of an API without influencing their pharmacological properties. The improved solubility and permeability of the ACZ-PABA cocrystal motivated the development of a novel tablet formulation. The improved tabletability properties of ACZ-PABA cocrystal over ACZ, enabled the preparation of tablets by a cost-effective direct compression process. The novel ACZ-PABA cocrystal based tablet exhibited better *in-vitro* drug dissolution profile and more than doubled bioavailability in humans over the marketed formulation, without

507

508

unwanted side-effects. Thus, the prescribed dose of ACZ could be reduced by the use of cocrystal-

based formulation, leading to significant saving.

Acknowledgements

A.G. sincerely acknowledges the financial support from AICTE, Govt. of India, New Delhi

under Research Promotion Scheme (RPS) vide F.No.8-5/RIFD/RPS/Policy-1/2017-18. Authors

are thankful to Nakoda Chemicals Ltd. (Hyderabad, India) for providing the gift sample of ACZ.

Authors sincerely acknowledge the Department of Pharmaceutical Sciences and Technology and

Central Instrumentation Facility (CIF) of BIT Mesra, Ranchi for providing all the necessary

facilities. Authors are also thankful to Pharmaceutical Materials Science and Engineering

Laboratory, Department of Pharmaceutics, College of Pharmacy, University of Minnesota, United

States, for providing all necessary facilities for conducting Hygroscopicity and Tabletability study.

Authors are indeed thankful to the TAAB Biostudy Services, Kolkata, India for conducting sub-

chronic oral toxicity study and comparative oral bioavailability study.

Authors Information

Corresponding Author

Animesh Ghosh: Solid State Pharmaceutics Research Lab, Department of Pharmaceutical

Sciences and Technology, Birla Institute of Technology, Mesra, Ranchi – 835215, Jharkhand,

India.

E-mail: aghosh@bitmesra.ac.in

ORCID: 0000-0002-2990-4738

Changquan Calvin Sun: Pharmaceutical Materials Science and Engineering Laboratory,

Department of Pharmaceutics, College of Pharmacy, University of Minnesota, 9-127B Weaver-

Densford Hall, 308 Harvard Street S.E., Minneapolis, MN 55455, United States

Email: sunx0053@umn.edu

ORCID: 0000-0001-7284-5334

References

- Aitipamula, S., Banerjee, R., Bansal, A.K., Biradha, K., Cheney, M.L., Choudhury, A.R., Desiraju, G.R., Dikundwar, A.G., Dubey, R., Duggirala, N., Ghogale, P.P., Ghosh, S., Goswami, P.K., Goud, N.R., Jetti, R.R.K.R., Karpinski, P., Kaushik, P., Kumar, D., Kumar, V., Moulton, B., Mukherjee, A., Mukherjee, G., Myerson, A.S., Puri, V., Ramanan, A., Rajamannar, T., Reddy, C.M., Rodriguez-Hornedo, N., Rogers, R.D., Row, T.N.G., Sanphui, P., Shan, N., Shete, G., Singh, A., Sun, C.C., Swift, J.A., Thaimattam, R., Thakur, T.S., Kumar Thaper, R., Thomas, S.P., Tothadi, S., Vangala, V.R., Variankaval, N., Vishweshwar, P., Weyna, D.R., Zaworotko, M.J., 2012. Polymorphs, Salts, and Cocrystals: What's in a Name? Cryst Growth Des 12, 2147–2152. https://doi.org/10.1021/cg3002948
- Aitipamula, S., Vangala, V.R., 2017. X-Ray Crystallography and its Role in Understanding the Physicochemical Properties of Pharmaceutical Cocrystals. J Indian Inst Sci 97, 227–243. https://doi.org/10.1007/s41745-017-0026-4
- Arenas-García, J.I., Herrera-Ruiz, D., Mondragón-Vásquez, K., Morales-Rojas, H., Höpfl, H., 2012. Modification of the Supramolecular Hydrogen-Bonding Patterns of Acetazolamide in the Presence of Different Cocrystal Formers: 3:1, 2:1, 1:1, and 1:2 Cocrystals from Screening with the Structural Isomers of Hydroxybenzoic Acids, Aminobenzoic Acids, Hydroxybenzamides, Aminobenzamides, Nicotinic Acids, Nicotinamides, and 2,3-Dihydroxybenzoic Acids. Cryst Growth Des 12, 811–824. https://doi.org/10.1021/cg201140g
- Arenas-García, J.I., Herrera-Ruiz, D., Mondragón-Vásquez, K., Morales-Rojas, H., Höpfl, H., 2010. Co-Crystals of Active Pharmaceutical Ingredients Acetazolamide. Cryst Growth Des 10, 3732–3742. https://doi.org/10.1021/cg1005693
- Arenas-García, J.I., Herrera-Ruiz, D., Morales-Rojas, H., Höpfl, H., 2017. Interrelation of the dissolution behavior and solid-state features of acetazolamide cocrystals. European Journal of Pharmaceutical Sciences 96, 299–308. https://doi.org/10.1016/j.ejps.2016.09.025
- Bolla, G., Nangia, A., 2016. Binary and ternary cocrystals of sulfa drug acetazolamide with pyridine carboxamides and cyclic amides. IUCrJ 3, 152–160. https://doi.org/10.1107/S2052252516000543
- Chow, S.F., Chen, M., Shi, L., Chow, A.H.L., Sun, C.C., 2012. Simultaneously Improving the Mechanical Properties, Dissolution Performance, and Hygroscopicity of Ibuprofen and Flurbiprofen by Cocrystallization with Nicotinamide. Pharm Res 29, 1854–1865. https://doi.org/10.1007/s11095-012-0709-5
- Dan, S., Chatterjee, N., Mandal, P., Das, A., Ghosh, B., Kumar Pal, T., 2016. Repeated dose Toxicity Study in Rats of the Formulation Containing Metformin and Sitagliptin using Microwave Assisted Acrylamide Grafted Cassia tora as Polymer. Nat Prod J 6, 152–160.
- Di Martino, P., Scoppa, M., Joiris, E., Palmieri, G.F., Andres, C., Pourcelot, Y., Martelli, S., 2001. The spray drying of acetazolamide as method to modify crystal properties and to improve compression behaviour. Int J Pharm 213, 209–221. https://doi.org/10.1016/S0378-5173(00)00675-X
- Duggirala, N.K., Perry, M.L., Almarsson, Ö., Zaworotko, M.J., 2016. Pharmaceutical cocrystals: along the path to improved medicines. Chemical Communications 52, 640–655. https://doi.org/10.1039/C5CC08216A
- El-Gazayerly, O.N., Hikal, A.H., 1997. Preparation and evaluation of acetazolamide liposomes as an ocular delivery system. Int J Pharm 158, 121–127. https://doi.org/10.1016/S0378-5173(97)00186-5

- Fang, J., Zhang, Z., Bo, Y., Xue, J., Wang, Y., Liu, J., Qin, J., Hong, Z., Du, Y., 2021. Vibrational spectral and structural characterization of multicomponent ternary co-crystal formation within acetazolamide, nicotinamide and 2-pyridone. Spectrochim Acta A Mol Biomol Spectrosc 245, 118885. https://doi.org/10.1016/j.saa.2020.118885
- Ghadi, R., Dand, N., 2017. BCS class IV drugs: Highly notorious candidates for formulation development. Journal of Controlled Release 248, 71–95. https://doi.org/10.1016/j.jconrel.2017.01.014
- Granero, G.E., Longhi, M.R., Becker, C., Junginger, H.E., Kopp, S., Midha, K.K., Shah, V.P., Stavchansky, S., Dressman, J.B., Barends, D.M., 2008. Biowaiver Monographs for Immediate Release Solid Oral Dosage Forms: Acetazolamide. J Pharm Sci 97, 3691–3699. https://doi.org/10.1002/jps.21282
- Granero, Gladys E., Maitre, M.M., Garnero, C., Longhi, M.R., 2008. Synthesis, characterization and in vitro release studies of a new acetazolamide–HP-β-CD–TEA inclusion complex. Eur J Med Chem 43, 464–470. https://doi.org/10.1016/j.ejmech.2007.03.037
- Haznedar, S., Dortunç, B., 2004. Preparation and in vitro evaluation of Eudragit microspheres containing acetazolamide. Int J Pharm 269, 131–140. https://doi.org/10.1016/j.ijpharm.2003.09.015
- Hu, S., Wang, C., He, X., Sun, C.C., 2020. Reducing the Sublimation Tendency of Ligustrazine through Salt Formation. Cryst Growth Des 20, 2057–2063. https://doi.org/10.1021/acs.cgd.9b01704
- Huang, L., 2004. Impact of solid state properties on developability assessment of drug candidates. Adv Drug Deliv Rev 56, 321–334. https://doi.org/10.1016/j.addr.2003.10.007
- Ji, X., Wu, D., Li, C., Li, J., Sun, Q., Chang, D., Yin, Q., Zhou, L., Xie, C., Gong, J., Chen, W., 2022. Enhanced Solubility, Dissolution, and Permeability of Abacavir by Salt and Cocrystal Formation. Cryst Growth Des 22, 428–440. https://doi.org/10.1021/acs.cgd.1c01051
- Kakkar, S., Bhattacharya, B., Reddy, C.M., Ghosh, S., 2018. Tuning mechanical behaviour by controlling the structure of a series of theophylline co-crystals. CrystEngComm 20, 1101–1109. https://doi.org/10.1039/C7CE01915G
- Kale, D.P., Zode, S.S., Bansal, A.K., 2017. Challenges in Translational Development of Pharmaceutical Cocrystals. J Pharm Sci 106, 457–470. https://doi.org/10.1016/j.xphs.2016.10.021
- Karki, S., Friščić, T., Fábián, L., Laity, P.R., Day, G.M., Jones, W., 2009. Improving Mechanical Properties of Crystalline Solids by Cocrystal Formation: New Compressible Forms of Paracetamol. Advanced Materials 21, 3905–3909. https://doi.org/10.1002/adma.200900533
- Kaur, I.P., Smitha, R., Aggarwal, D., Kapil, M., 2002. Acetazolamide: future perspective in topical glaucoma therapeutics. Int J Pharm 248, 1–14. https://doi.org/10.1016/S0378-5173(02)00438-6
- Koranne, S., Krzyzaniak, J.F., Luthra, S., Arora, K.K., Suryanarayanan, R., 2019. Role of Coformer and Excipient Properties on the Solid-State Stability of Theophylline Cocrystals. Cryst Growth Des 19, 868–875. https://doi.org/10.1021/acs.cgd.8b01430
- Kumari, N., Bhattacharya, B., Roy, P., Michalchuk, A.A.L., Emmerling, F., Ghosh, A., 2019. Enhancing the Pharmaceutical Properties of Pirfenidone by Mechanochemical Cocrystallization. Cryst Growth Des 19, 6482–6492. https://doi.org/10.1021/acs.cgd.9b00932

- Kumari, N., Ghosh, A., 2020. Cocrystallization: Cutting Edge Tool for Physicochemical Modulation of Active Pharmaceutical Ingredients. Curr Pharm Des 26, 4858–4882. https://doi.org/10.2174/1381612826666200720114638
- Manin, A.N., Drozd, K. V., Surov, A.O., Churakov, A. V., Volkova, T. V., Perlovich, G.L., 2020. Identification of a previously unreported co-crystal form of acetazolamide: a combination of multiple experimental and virtual screening methods. Physical Chemistry Chemical Physics 22, 20867–20879. https://doi.org/10.1039/D0CP02700F
- Meers, K.J., Tran, T.N., Zheng, Q., Unruh, D.K., Hutchins, K.M., 2020. Hydrogen-Bond Synthon Preferences in Cocrystals of Acetazolamide. Cryst Growth Des 20, 5048–5060. https://doi.org/10.1021/acs.cgd.0c00210
- Pandey, N., Ghosh, A., 2022. An outlook on permeability escalation through cocrystallization for developing pharmaceuticals with improved biopharmaceutical properties. J Drug Deliv Sci Technol 76, 103757. https://doi.org/10.1016/j.jddst.2022.103757
- Roy, P., Chakraborty, S., Pandey, N., Kumari, N., Chougule, S., Chatterjee, A., Chatterjee, K., Mandal, P., Gorain, B., Dhotre, A. V., Bansal, A.K., Ghosh, A., 2023. Study on Sulfamethoxazole–Piperazine Salt: A Mechanistic Insight into Simultaneous Improvement of Physicochemical Properties. Mol Pharm 20, 5226–5239. https://doi.org/10.1021/acs.molpharmaceut.3c00646
- Roy, P., Ghosh, A., 2020. Progress on cocrystallization of poorly soluble NME's in the last decade. CrystEngComm 22, 6958–6974. https://doi.org/10.1039/D0CE01276A
- Roy, P., Pandey, N., Ghosh, A., 2022. Molecular Docking of Pharmaceutical Cocrystal As a Ligand: Do We Need to Rethink? Crystal Growth & Design 0. https://doi.org/10.1021/acs.cgd.2c01379
- Schultheiss, N., Newman, A., 2009. Pharmaceutical Cocrystals and Their Physicochemical Properties. Cryst Growth Des 9, 2950–2967. https://doi.org/10.1021/cg900129f
- Silchenko, S., Nessah, N., Li, J., Li, L.-B., Huang, Y., Owen, A.J., Hidalgo, I.J., 2020. In vitro dissolution absorption system (IDAS2): Use for the prediction of food viscosity effects on drug dissolution and absorption from oral solid dosage forms. European Journal of Pharmaceutical Sciences 143, 105164. https://doi.org/10.1016/j.ejps.2019.105164
- Singh, G.K., Kumar, V., 2011. Acute and sub-chronic toxicity study of standardized extract of Fumaria indica in rodents. J Ethnopharmacol 134, 992–995. https://doi.org/10.1016/j.jep.2011.01.045
- Song, S., Wang, C., Wang, S., Siegel, R.A., Sun, C.C., 2021. Efficient development of sorafenib tablets with improved oral bioavailability enabled by coprecipitated amorphous solid dispersion. Int J Pharm 610, 121216. https://doi.org/10.1016/j.ijpharm.2021.121216
- Song, Y., Wang, L.-Y., Liu, F., Li, Y.-T., Wu, Z.-Y., Yan, C.-W., 2019. Simultaneously enhancing the *in vitro / in vivo* performances of acetazolamide using proline as a zwitterionic coformer for cocrystallization. CrystEngComm 21, 3064–3073. https://doi.org/10.1039/C9CE00270G
- Soni, S.R., Bhunia, B.K., Kumari, N., Dan, S., Mukherjee, S., Mandal, B.B., Ghosh, A., 2018. Therapeutically Effective Controlled Release Formulation of Pirfenidone from Nontoxic Biocompatible Carboxymethyl Pullulan-Poly(vinyl alcohol) Interpenetrating Polymer Networks. ACS Omega 3, 11993–12009. https://doi.org/10.1021/acsomega.8b00803
- Sun, C.C., 2010. Setting the bar for powder flow properties in successful high speed tableting. Powder Technol 201, 106–108. https://doi.org/10.1016/j.powtec.2010.03.011

- Sun, C.C., 2009. Materials Science Tetrahedron—A Useful Tool for Pharmaceutical Research and Development. J Pharm Sci 98, 1671–1687. https://doi.org/10.1002/jps.21552
- van Breemen, R.B., Li, Y., 2005. Caco-2 cell permeability assays to measure drug absorption. Expert Opin Drug Metab Toxicol 1, 175–185. https://doi.org/10.1517/17425255.1.2.175
- Verma, P., Gupta, R.N., Jha, A.K., Pandey, R., 2013. Development, *in vitro* and *in vivo* characterization of Eudragit RL 100 nanoparticles for improved ocular bioavailability of acetazolamide. Drug Deliv 20, 269–276. https://doi.org/10.3109/10717544.2013.834417
- Vreeman, G., Sun, C.C., 2021. Mean yield pressure from the in-die Heckel analysis is a reliable plasticity parameter. Int J Pharm X 3, 100094. https://doi.org/10.1016/j.ijpx.2021.100094
- Wang, C., Hu, S., Sun, C.C., 2017. Expedited Development of Diphenhydramine Orally Disintegrating Tablet through Integrated Crystal and Particle Engineering. Mol Pharm 14, 3399–3408. https://doi.org/10.1021/acs.molpharmaceut.7b00423
- Wang, C., Song, S., Gunawardana, C.A., Sun, D.J., Sun, C.C., 2022. Effects of shear cell size on flowability of powders measured using a ring shear tester. Powder Technol 396, 555–564. https://doi.org/10.1016/j.powtec.2021.11.015
- Wang, K., Hao, Y., Wang, C., Zhao, X., He, X., Sun, C.C., 2022. Simultaneous improvement of physical stability, dissolution, bioavailability, and antithrombus efficacy of Aspirin and Ligustrazine through cocrystallization. Int J Pharm 616, 121541. https://doi.org/10.1016/j.ijpharm.2022.121541
- Wong, S.N., Chen, Y.C.S., Xuan, B., Sun, C.C., Chow, S.F., 2021. Cocrystal engineering of pharmaceutical solids: therapeutic potential and challenges. CrystEngComm 23, 7005–7038. https://doi.org/10.1039/D1CE00825K
- Yasmin, S., Cerchia, C., Badavath, V.N., Laghezza, A., Dal Piaz, F., Mondal, S.K., Atlı, Ö., Baysal, M., Vadivelan, S., Shankar, S., Siddique, M.U.M., Pattnaik, A.K., Singh, R.P., Loiodice, F., Jayaprakash, V., Lavecchia, A., 2021. A Series of Ferulic Acid Amides Reveals Unexpected Peroxiredoxin 1 Inhibitory Activity with in vivo Antidiabetic and Hypolipidemic Effects. ChemMedChem 16, 484–498. https://doi.org/10.1002/cmdc.202000564
- Yousef, M.A.E., Vangala, V.R., 2019. Pharmaceutical Cocrystals: Molecules, Crystals, Formulations, Medicines. Cryst Growth Des 19, 7420–7438. https://doi.org/10.1021/acs.cgd.8b01898
- Zhang, Y.-X., Wang, L.-Y., Dai, J.-K., Liu, F., Li, Y.-T., Wu, Z.-Y., Yan, C.-W., 2019. The comparative study of cocrystal/salt in simultaneously improving solubility and permeability of acetazolamide. J Mol Struct 1184, 225–232. https://doi.org/10.1016/j.molstruc.2019.01.090
- Zhou, Q., Shi, L., Chattoraj, S., Sun, C.C., 2012. Preparation and Characterization of Surface-Engineered Coarse Microcrystalline Cellulose Through Dry Coating with Silica Nanoparticles. J Pharm Sci 101, 4258–4266. https://doi.org/10.1002/jps.23301
- Zhou, Q., Shi, L., Marinaro, W., Lu, Q., Sun, C.C., 2013. Improving manufacturability of an ibuprofen powder blend by surface coating with silica nanoparticles. Powder Technol 249, 290–296. https://doi.org/10.1016/j.powtec.2013.08.031